Multiplicity dependence of hyperon and hypertriton production in Zr+Zr and Ru+Ru collisions at $\sqrt{s_{NN}}$ = 200 GeV

Dongsheng Li[1,*] (for the STAR collaboration)

[1]University of Science and Technology of China

Abstract. We present yield measurements on hyperons ($\Lambda, \overline{\Lambda}$ and $\Xi^-, \overline{\Xi}^+$) and hypertriton ($^3_\Lambda$H, $^3_{\overline{\Lambda}}\overline{\text{H}}$) in four different centrality classes of Zr+Zr and Ru+Ru collisions at $\sqrt{s_{\text{NN}}}$ = 200 GeV. The yield ratios of Λ/π^-, Ξ^-/π^-, $^3_\Lambda$H/Λ and S_3 = ($^3_\Lambda$H/Λ)/(^{3}He/p) are reported as a function of multiplicity, while the ratio of $^3_\Lambda$H/^{3}He is reported as a function of p_{T} in each centrality. The comparisons between data and models are discussed. These results provide insights on particle production mechanisms in heavy-ion collisions.

1 Introduction

In analogy to the Big Bang theory, which describes the origin and evolution of the universe, high energy heavy-ion collisions (HIC) can be dubbed the Little Bang. Although they are different systems, measurements on particle production in HIC would possibly help us understand the first few minutes of the evolution of our universe.

Recently, the dependence of particle production in HIC on system size has drawn a lot of attention [1–10, 15]. For hadron production, such dependence mainly reflects the properties of the hot medium. While for large nuclear clusters like hypertriton ($^3_\Lambda$H), their internal structures might also leave some non-negligible fingerprints on the yields, because their nuclear size are of the same magnitude as the size of the fireball created in the collisions and may be even larger than the fireball size for some small collision systems. These studies aim to verify our understanding of particle production mechanisms in HIC.

2 Results and discussions

In system size studies, the charged-particle multiplicity within unit of pseudo-rapidity $\langle \text{dN}_{\text{ch}}/\text{d}\eta \rangle$ is usually suggested as a measure of system size. In this work, we report the multiplicity dependence of hyperon and $^3_\Lambda$H production in Zr+Zr and Ru+Ru collisions at $\sqrt{s_{\text{NN}}}$ = 200 GeV, by analysing about 3.7 billion minimum bias events. These short-lived particles are reconstructed in STAR with the KFParticle Package [16], using the 2-body decay channels including $\Lambda \rightarrow \text{p} + \pi^-$, $\Xi^- \rightarrow \Lambda + \pi^-$, $^3_\Lambda\text{H} \rightarrow {}^3\text{He} + \pi^-$ and their charge conjugates within the mid-rapidity (|y| < 0.5 for (anti)hyperon, |y| < 0.8 for (anti)hypertriton). The daughter particle tracks including $\pi^\pm$, p($\overline{\text{p}}$), ^{3}He($^3\overline{\text{He}}$) are identified with energy loss $\langle \text{dE/dx} \rangle$ and momentum information measured by the Time Projection Chamber (TPC). The production yields are measured and the systematic uncertainties include components from tracking efficiency, topological cut variation, MC weighting and extrapolation.

*e-mail: erl@mail.ustc.edu.cn

2.1 Hyperon-to-pion ratio

In Fig. 1, hyperon-to-pion ratios are shown as a function of multiplicity, where the solid markers show the results from this study, while open markers show results from other collision systems [1–5, 11, 12]. In this analysis, the feed-down contributions from weak decay have been subtracted for Λ and $\overline{\Lambda}$, while for Ξ^- and $\overline{\Xi}^+$ such contributions are negligible. The yield ratios have similar values for the systems with similar multiplicity, which means that the strangeness production mechanisms are similar despite differences in the collision energies and the beam particle species. These yield ratios show a slightly increasing trend from small to large systems and such enhancement is usually considered as a signature of QGP formation in large systems.

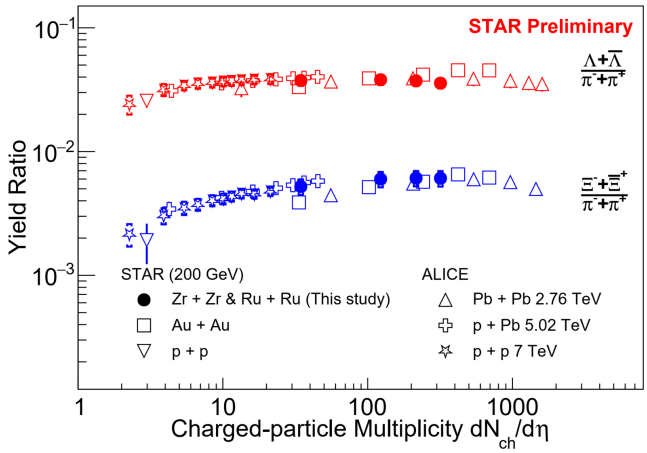

Figure 1. The hyperon-to-pion ratios as a function of charged-particle multiplicity. Yields of particles are combined with those of anti-particles. Red markers show the $(\Lambda + \overline{\Lambda})/(\pi^- + \pi^+)$ ratio, while blue markers show the $(\Xi^- + \overline{\Xi}^+)/(\pi^- + \pi^+)$ ratio, respectively [1–5, 11, 12].

2.2 ${}^3_\Lambda\mathrm{H}/\Lambda$ and S_3 ratios

The light hypernuclei production mechanisms in HIC are still not fully understood. The yield ratios of ${}^3_\Lambda\mathrm{H}/\Lambda$ and $S_3 = ({}^3_\Lambda\mathrm{H}/\Lambda)/({}^3\mathrm{He/p})$ are suggested as probes to distinguish different production mechanisms. Measurements on these hypernuclei yield ratios are shown in Fig. 2. In this analysis, the yields of Λ, proton and ^{3}He are corrected for feed-down from weak decay channels. Predictions from several popular theoretical models are also shown for comparison. The thermal model calculations are generated with canonical ensemble using the Thermal-Fist package [17]. The thermal model parameters for Zr+Zr and Ru+Ru collisions are obtained by fitting the yields of light hadrons, including $\pi^\pm$, $K^\pm$, p, $\Lambda(\bar{\Lambda})$ and $\Xi^-(\bar{\Xi}^+)$, in each centrality interval. The correlation volume (V_c) is varied from $V_c = dV/dy$ to $3dV/dy$. Other thermal model parameters are varied by 1-σ to generate the uncertainty bands. The thermal model predictions for LHC energies are directly taken from [15]. The analytical coalescence model calculations are generated with several assumptions of a thermalized hadron emission source, using both 2-body and 3-body Wigner functions to treat the nucleon coalescence process [18]. We also compared it with another coalescence model that applies the MUSIC and UrQMD models to simulate the QGP evolution and hadronic rescattering before the coalescence. Subsequently, it uses the 3-body Wigner function with different inputs of the Λ binding energy (B_Λ) of ${}^3_\Lambda\mathrm{H}$ for the coalescence afterburner [19].

The S_3 ratio in this study is roughly consistent with that in Au+Au and U+U collisions [13]. The ${}^3_\Lambda\mathrm{H}/\Lambda$ and S_3 ratios from this study and from the ALICE collaboration

measurements [14, 15] show similar trends. These results strongly deviate from the thermal model predictions, while agreeing with calculations by coalescence model of certain configurations. In particular, we find that the MUSIC + UrQMD + Coal. model with B_Λ = 0.42 MeV [20] can simultaneously describe both yield ratios well. However, we note that the B_Λ averaged over all current measurements is 0.164 ± 0.043 MeV, which is significantly smaller than 0.42 MeV. An increasing trend from small to large collision systems is observed in the ${}^3_\Lambda\mathrm{H}/\Lambda$ ratio, which is understood as a result of canonical suppression and possibly also the large nuclear size of ${}^3_\Lambda\mathrm{H}$. While for the S_3 ratio, a much weaker multiplicity dependence is observed compared to the ${}^3_\Lambda\mathrm{H}/\Lambda$ ratio, which is possibly due to the nuclear size effect since the conserved charges like baryon number and strangeness number all cancel out.

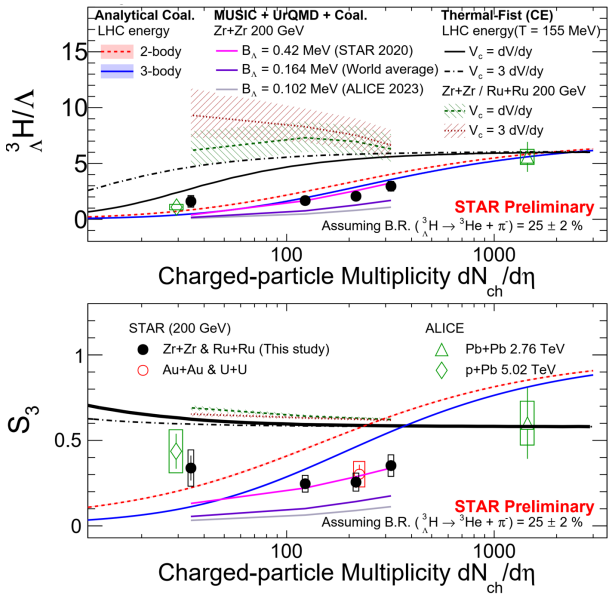

Figure 2. The multiplicity dependence of ${}^3_\Lambda\mathrm{H}/\Lambda$ and S_3. Solid circles show results from 200 GeV Zr+Zr and Ru+Ru collisions by this study, while open markers show results from other collision systems. Different model calculations are shown for comparison, including the analytical coalescence model (red and blue shaded bands), MUSIC + UrQMD + Coal. model of different Λ binding energy inputs (magenta, violet and grey lines) and Thermal-Fist model with the canonical ensemble assumption (black lines, green and brown shaded bands).

2.3 ${}^3_\Lambda\mathrm{H}/{}^3\mathrm{He}$ ratio

The constituents of ${}^3_\Lambda\mathrm{H}$ would be the same as those of ^{3}He if one substitutes the Λ with a proton. Although their masses are very similar, they have very different sizes. The nuclear radius of ${}^3_\Lambda\mathrm{H}$ is $\sim$ 5 fm, while that of ^{3}He is $\sim$ 2 fm, thus the coalescence model expects a strong multiplicity dependence and a p_T softening of the ${}^3_\Lambda\mathrm{H}/{}^3\mathrm{He}$ ratio [19]. While in the thermal model, all particles are generally treated point-like with no internal structure.

In Fig. 3, the ${}^3_\Lambda\mathrm{H}/{}^3\mathrm{He}$ ratio is measured in different centrality classes of Zr+Zr and Ru+Ru collisions, showing a weak p_T and multiplicity dependence. By comparing with the model predictions, it seems our data points are roughly described by the coalescence model with B_Λ= 0.42 MeV, while overestimated by the thermal model. Again, we note that this value seems to be large compared with the world average value.

3 Summary and outlook

The yield measurements on hyperons ($\Lambda, \overline{\Lambda}$ and $\Xi^-, \overline{\Xi}^+$) and hypertriton (${}^3_\Lambda\mathrm{H}, {}^3_{\overline{\Lambda}}\overline{\mathrm{H}}$) in Zr+Zr and Ru+Ru collisions at $\sqrt{s_\mathrm{NN}}$ = 200 GeV are reported. The multiplicity dependence of

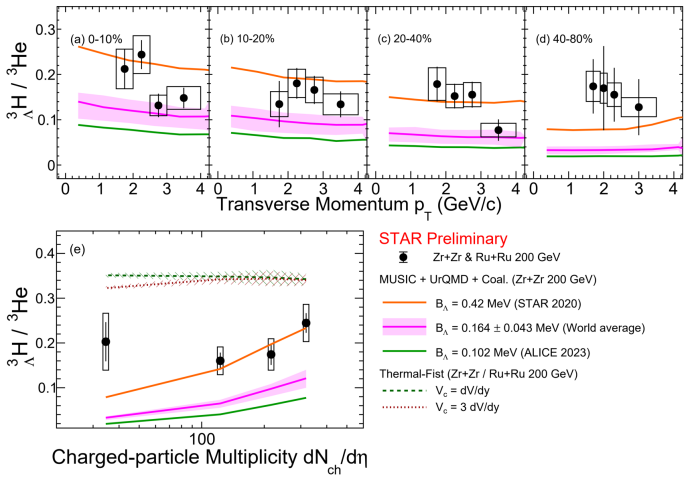

Figure 3. Fig.(a) - Fig.(d) show the p_T dependence of $^3_\Lambda$H/^{3}He, while Fig(e) shows the multiplicity dependence of the p_T integrated ratio. Black points show the measurement in this study. Model predictions from MUSIC + UrQMD + Coal. model of different Λ binding energy inputs are shown as orange, magenta and green lines, while Thermal-Fist are shown as the green and brown shaded bands.

hyperon and light hypernuclei production are investigated. It is found that the hyperon production mechanisms are similar in systems with the same multiplicity, despite differences of the collision energies and the beam particle species. For light hypernuclei production, the measurements roughly agree with certain coalescence model predictions and strongly deviate from the thermal model calculations. However, the coalescence model with the world average measured B_Λ does not describe the data well. Thus, more efforts from the theoretical side, as well as higher precision measurements in small systems will be necessary to elucidate the role of the nuclear size on the formation of light hypernuclei in HIC.

References

[1] J. Adams et al. (STAR collaboration), Phys. Rev. Lett. **98** (2007), 062301. https://doi.org/10.1103/PhysRevLett.98.062301

[2] B. B. Abelev et al. (ALICE collaboration), Phys. Lett. B **728** (2014), 216-227. https://doi.org/10.1016/j.physletb.2014.05.052 [erratum: Phys. Lett. B **734** (2014), 409-410. https://doi.org/10.1016/j.physletb.2014.05.052]

[3] B. B. Abelev et al. (ALICE collaboration), Phys. Lett. B **728** (2014), 25-38. https://doi.org/10.1016/j.physletb.2013.11.020]

[4] J. Adam et al. (ALICE collaboration), Phys. Lett. B **758** (2016), 389-401. https://doi.org/10.1016/j.physletb.2016.05.027

[5] J. Adam et al. (ALICE collaboration), Nature Phys. **13** (2017), 535-539. https://doi.org/10.1038/nphys4111

[6] S. Acharya et al. (ALICE collaboration), Eur. Phys. J. C **80** (2020) no.9, 889. https://doi.org/10.1140/epjc/s10052-020-8256-4

[7] S. Acharya et al. (ALICE collaboration), Phys. Rev. C **101** (2020) no.4, 044906. https://doi.org/10.1103/PhysRevC.101.044906

[8] S. Acharya et al. (ALICE collaboration), Phys. Lett. B **800** (2020), 135043. https://doi.org/10.1016/j.physletb.2019.135043

[9] S. Acharya et al. (ALICE collaboration), Phys. Lett. B **794** (2019), 50-63. https://doi.org/10.1016/j.physletb.2019.05.028

[10] J. H. Chen, X. Dong, X. H. He, H. Z. Huang, F. Liu et al. arXiv:2407.02935. https://doi.org/10.48550/arXiv.2407.02935

[11] B. I. Abelev et al. (STAR collaboration), Phys. Rev. C **75** (2007), 064901. https://doi.org/10.1103/PhysRevC.75.064901

[12] B. I. Abelev et al. (STAR collaboration), Phys. Rev. C **79** (2009), 034909. https://doi.org/10.1103/PhysRevC.79.034909

[13] M. I. Abdulhamid, et al. (STAR collaboration), Nature **632** (2024), 1026–1031. https://doi.org/10.1038/s41586-024-07823-0

[14] J. Adam et al. (ALICE collaboration), Phys. Lett. B **754** (2016), 360-372. https://doi.org/10.1016/j.physletb.2016.01.040

[15] S. Acharya et al. (ALICE collaboration), Phys. Rev. Lett. **128** (2022) no.25, 252003. https://doi.org/10.1103/PhysRevLett.128.252003

[16] X. Y. Ju, Y. H. Leung, S. Radhakrishnann et al., Nucl. Sci. Tech. **34** (2023) 158. https://doi.org/10.1007/s41365-023-01320-1

[17] V. Vovchenko and H. Stoecker, Comput. Phys. Commun. **244** (2019), 295-310. https://doi.org/10.1016/j.cpc.2019.06.024

[18] K. J. Sun, C. M. Ko and B. Dönigus, Phys. Lett. B **792** (2019), 132-137. https://doi.org/10.1016/j.physletb.2019.03.033

[19] D. N. Liu, C. M. Ko, Y. G. Ma, F. Mazzaschi, M. Puccio, Q. Y. Shou, K. J. Sun and Y. Z. Wang, Phys. Lett. B **855** (2024), 138855. https://doi.org/10.1016/j.physletb.2024.138855

[20] J. Adam et al. (STAR Collaboration) Nature Phys. **16** (2020) 4, 409-412. https://doi.org/10.1038/s41567-020-0799-7